Submitted for publication in ApJ
Preprint typeset using LaTeX style emulateapj v. 01/23/15

THE SPATIAL DISTRIBUTION OF LOCAL GROUP SATELLITES IN A COSMOLOGICAL CONTEXT

Verónica Arias [1], Jaime E. Forero-Romero [2]
[1]Departamento de Física, Universidad de los Andes, Cra. 1 No. 18A-10, Edificio Ip, Bogotá, Colombia

Submitted for publication in ApJ

ABSTRACT

We focus on the spatial distribution of bright ($M_V < -8$) satellites and pairs of galaxies with similar masses, isolation and kinematic configurations as the Local Group.

Subject headings: Galaxies: halos — Galaxies: high-redshift — Galaxies: statistics — Dark Matter — Methods: numerical

1. INTRODUCTION

Since the early works of (el que libeskind dice que habl de eso primero) and Lynden-Bell (1976), the observed anisotropic distribution of satellite galaxies in the Local Group has been a key point in the discussion of galaxy formation models within ΛCDM cosmology. These pioneer papers described that the then known satellite galaxies of the Milky May (MW) were distributed roughly following the plane that contained the Magelanic clouds and their stellar tails. This anisotropic distribution was further studied in the work of Pawlowski et. al. (2012), where they included all the known MW satellite galaxies (XXX more than in the original Lynden-Bell paper) as well as some MW globular clusters, and found that they are all contained in what they call a "Vast Plane Of Satellites" (VPOS). This structure is around 30kpc thick and is perpendicular to the stellar disc of the MW galaxy. This plane of satellites was considered a rarity until the PAndAS survey of the Andromeda (M31) galaxy and its halo (missing reference on the survey) provided a complete sample of the satellite galaxy population (above a XXXX magnitude) of our neighboring galaxy, allowing their consistent distance estimations (Conn et al. 2012). In a groundbreaking work, Ibata et al. (2013) found that 15 out of the 30 satellites are in a planar structure that is 15kpc thick and has an extension of 400kpc. Additionally, from line of sight velocity measurements, they found that the structure has an apparent coherent rotation, with the satellites south of M31 moving away from us and those north of M31 coming towards us. This apparent organized rotation of satellite galaxies was also statistically found to occur in diametrically opposed pairs of satellites from the SDSS (Ibata et al. 2014), although this results were contested in a follow up paper by Cuatun et al. (2014).

These discoveries of the planes in M31 and the MW were followed by the remark from Shaya et al. (2013) that the other satellite galaxies in M31 could be part of a second plane, further reinforcing the idea that satellites in the local group are not isotropically distributed. Despite the challenges in estimating distances to the satellites galaxies, Tully et al. managed to go beyond the local group and found two planes of satellites galaxies in Centaurus A, making a clearer case for the planes of satellites: in all the galaxies where distance measurements could be performed evidence of satellite planar structures have been found.

These observed planes and their apparent co-rotation seem to challenge current galaxy formation models (Pawlowski et al. 2014). Pawlowski et al. (2012) compared the kinematic structure of the MW satellites against DM only simulation of high resolution halos from the Via Lactea and Aquarius projects and could not find find a similar kinematic structure (i.e. the orbital poles of the MW satellites) in the simulations. Additionally, a few months after the discovery of the M31 plane of satellites, Bahl and Baumgardt (2013) looked for similar structures in the MilleniummII dark matter only cosmological simulations, and found that planar structures are common (they found them in around 2 per cent of host halos). Nevertheless these results were contradicted by the works of Ibata el al. (2014) and Pawlowski et al. (2014) who, analyzing the same cosmological simulations with methods closer to those used to analyze the observational data, found that planar structures such as that observed in M31 are extremely rare (less than 0.02 per cent or 0.004 per cent respectively). But satellite galaxies are not particularly good tracers of the underlying dark matter structure (Sawala 2014), and indeed anisotropic distributions of the satellites have been found in the APOSTOLE simulations that include baryonic physics (Sawala et al. 2016), although the Milky Way remains an extreme case. These results were contested by Pawlowski et al. (2015) who claim that the anisotropies found are a product of using a metric that ignores the radial position of the galaxies. In CLUES, a high resolution constrained Local Group simulation, Gillet et al. (2015) found M31-like planes but again, the observed M31 plane remains an extreme case, and this seems to be corroborated by Cautun et al. (2015), who, despite finding a great variety of planes in simulations remarks that the observed M31 plane has an "unusually large radial extent".

In addition to these plane-finding efforts in cosmological simulations, many works have focused on the possible formation processes that led to planar structures and on the alignments of these structures with the cosmic web. In a pioneer work Libeskind et al. (2011) measured the infall direction of satellites in a DM only constrained simulation of one pair of LG halos and found that there is a definite infall direction. Using cosmological dark

matter only simulations Libeskind et al. (2014) showed that the preferential infall direction was along cosmic filaments, result that was also obtained by Lee & Choi (2015). This result was further confirmed by Tempel et al. (2015), who measure the angle between satellites and the direction defined by filaments (Bissous filament finder) to find a signal both in the SDSS galaxy catalog and in the semi-analytic galaxies in the Millennium Simulation. Additionally, an analysis of the cosmic flow data set by Libeskind et al. (2015) reveals that four out of the fives satellite planes observed in the Local Group are aligned with a filament. Additionally, Libeskind et al. (2016) use the SDSS DR10 catalog to study galaxy pairs and find that satellites tend to accumulate towards the companion galaxy: There are up to $\sim 10\%$ more satellites in the space between the pair than expected from an uniform distribution.

Early filamentary accretion has been proposed as the formation mechanism for the Andromeda thin plane of satellites (Buck et al 2015), with early formed galaxies accreting their mass via cold thin filaments. This formation mechanism results naturally in thin planes, but a follow up work shows that these are not kinematically coherent structures (Buck et al. 2015). These results are from dark matter only simulations, so it would be interesting to see if they still hold for simulations that include baryonic physics, since it was shown by Gonzales et al 2015 that satellites accreted via filaments are destroyed faster than those that are not. So far, the planes found in simulations tend to be transient structures (XXXXXXX) and that poses two problems: one is why do we see planes in all the three galaxies were we can actually make the measurements if they are transient? The second is that these findings seem to be at odds with the observed rotational coherence of the MW satellites for which proper motion measurements exist (Pawlowski et al. 2015).

In a more general numerical study, Shao et al. (2016) use the EAGLE simulation to study the alignment of satellites with respect to the central galaxy. They find a weak alignment. Around 20% of the systems have a misalignment angle larger than the value observed for the Milky Way. In this work, we continue these approach of studying more generally the alignments between the satellites population, the dark matter substructures and the main host halos in the illustris simulation. This paper is organized as follows. In Section 2 we describe the numerical setup, the sample selection criteria, the method to determine the cosmic web environment and the method to quantify alignments. The alignments and lack thereof obtained are presented in Section 3 and compared with the Local Group observations. Finally, these results are discussed more broadly in Section 4.

2. NUMERICAL SETUP

2.1. *Illustris simulation*

In this work we use the publicly available results from the Illustris simulation (Vogelsberger et al. 2014). This cosmological simulation, performed using the quasi-Lagrangian code AREPO, follows the coupled evolution of dark matter and gas, and includes parametrizations to account for the effects of gas cooling, photoionization, star formation, stellar feedback, black hole and super massive black hole feedback. Vogelsberger et al. 2014 use a $75Mpc/h$ simulation box, with ΛCDM cosmology initial conditions starting at a redshift $z = 127$ and consistent with WMAP-9 measurments.

2.2. *Sample Selection*

We select all halos with maximum circular velocities in the range 150 km s^{-1} $< V_{\rm max} <$ 350 km s^1. We exclude sub-halos from this selection. From this set we construct a sample of pairs as follows. For each halo A we find its closest halo B, if halo A is also the closest to halo B, the two halos are considered as a pair. Another way to phrase this selection is that pairs do not have neighbors closer than the pair's distance. We exclude the pairs that are closer than There are 53 pairs with those conditions in the simulation.

We extract from the simulation spheres of 2 h^{-1}Mpcin radius around the pair's center of mass. We use this information to exclude all the pairs that have separations smaller than the sum of their virial radii, i.e. we exclude interacting pairs. This reduces to 49 the number of pairs in the sample.

We count the number of galaxies with $M_V < -9$ inside the virial radius of each halo, including the central galaxy. We only keep pairs where both halos have 5 bright galaxies at least. This reduces the sample to 24 pairs. We call this sample the Full Sample.

From the Full Sample we build a second sample based on the pairs' kinematics. Figure 1 shows the co-moving separation and relative speed between the two halos in the pair. The stars in the Figure represent the pairs with a separation in the range $0.75h^{-1}$Mpc $< R_{AB} <$ $1.50h^{-1}$Mpc and relative velocity in the range $V_{AB} > 100$ km s^{-1}, which are close to the Local Group Observed values. We call this sample the LG Sample.

The number of pairs in the Full Sample is consistent with previous calculations. Forero-Romero et al. (2013) performed a study of the LG kinematics using a cosmological N-body simulation as a benchmark. In their study, using criteria similar to ours to define the Full Sample, they found 1923 pairs in a volume of 250^3 h^{-3} Mpc^3. With the same number density we expect to find 52 pairs in the volume of the Illustris simulation, which is very close to the actual number of 49 pairs.

In the same study they found 158 pairs with broad kinematic characteristics, similar to the definition of our LG sample. This represents a reduction of a factor of 12 from their General Sample. With those numbers in mind we would expect to keep at least 4 pairs in the Illustris volume. Given that our conditions are slightly more relaxed (we do not ask for isolation criteria from massive halos) we end up with a larger sample size, but still consistent with the fact that LG-like pairs are scarce.

2.3. *Cosmic Web environment*

We place the pairs in our sample into the cosmic web as quantified by the deformation tensor. (Hahn et al. 2007; Forero-Romero et al. 2009). This method computes a cartesian grid the tensor T_{ij},

$$T_{ij} \equiv \frac{\partial^2 \phi}{\partial r_i \partial r_j} \quad (1)$$

where ϕ is a pseudo-gravitational potential that follows the Poisson equation $\nabla^2 \phi = -\delta$ and the r_i coordinates

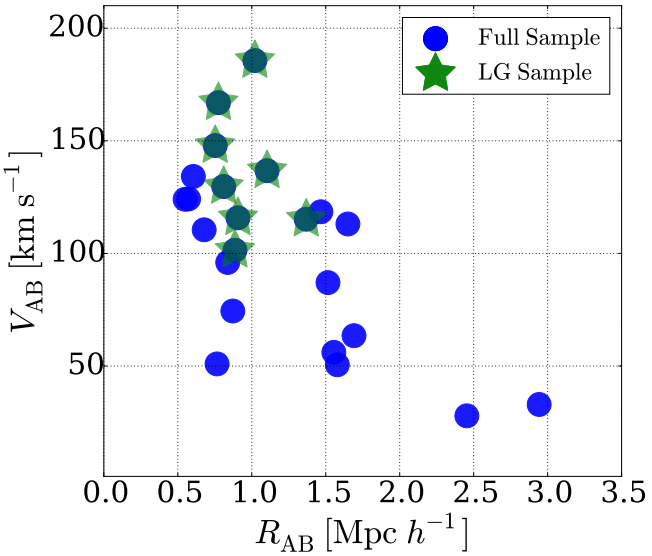

FIG. 1.— Halo pair samples used in this paper located in the plane of relative co-moving velocity V_{AB} versus relative distance R_{AB} between the two halos in the pair. The R&V sample is the closest to the separation and kinematic conditions observed in the Local Group.

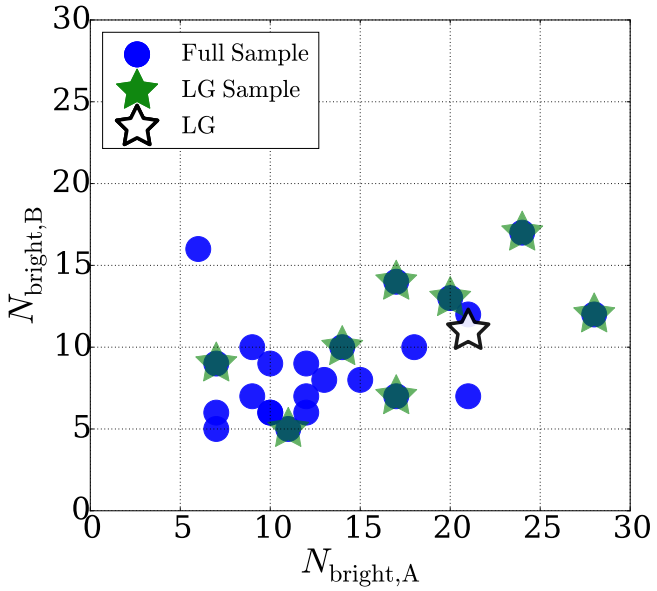

FIG. 2.— Number of bright substructures ($M_B < -9$) and dark matter substructures.

correspond to a cartesian system with $i = 1, 2, 3$.

This tensor is and symmetric and can be diagonalized. Its eigenvalues ($\lambda_1 > \lambda_2 > \lambda_3$) and corresponding eigenvectors ($\hat{e}_1$, $\hat{e}_2$, $\hat{e}_3$) define the degree and direction of stability around the neighborhood where the tensor was computed. This allows the classification of that region either as a peak, filaments, sheets and voids in the case of three, two, one or zero eigenvalues larger than a given threshold λ_{th}.

In this study we compute these eigenvalues and eigenvectors over the dark matter component of the Illustris-3 simulation on a cubic mesh of 74 cells on a side. This resolution corresponds to ~ 1 Mpc h. We interpolate the DM density on that mesh using a Cloud-In-Cell (CIC) scheme. We proceed to smooth the density field with a gaussian window with a physical scale equal to the cell size.

We choose this interpolation and smoothing scale for two reasons. First, because it corresponds to the typical pair separation in our sample. Second, because it allows a direct comparison with other results in the literature that used the same methodology to quantify the cosmic web environment for Local Group pairs in a cosmological context (Forero-Romero et al. 2013; Forero-Romero & González 2015).

2.4. *Characterization of spatial distributions*

In this paper, our main aim is to study alignments: of the satellite population with the cosmic web, of the dark matter halos with the axis that unites them, etc... To do this, we fitted a triaxial spheroid to both the satellite (bright) and the dark matter (dark) subhalo distributions, to get both their semi-major and semi-minor axis. With this geometrical information we can study the alignments of the two distributions with the cosmic web, and also with the vector that unites the halo pair that host these substructures. Additionally, we calculate the axis ratio of the distributions to determine its "flatness" and look for differences between dark and bright distributions and between substructure in the full sample and in the LG sample.

3. RESULTS

3.1. *Alignments of the galaxy pairs with the cosmic web*

Alignments between galaxies and the cosmic web were investigated by (Forero-Romero et al. 2013) who found that the axis that unites halo pairs similar to the MW-M31 pair tends to align with the $\hat{e}_3$ vector. We investigated this alignment on both our Full and LG samples. In Figure 3 we plot the integrated probability of the dot product between the $\hat{e}_3$ vector and the vector that unites the galaxy pair ($\hat{r}_{AB}$). This integrated probability shows that $\hat{e}_3$ and $\hat{r}_{AB}$ tend to be aligned, which is consistent with the literature results mentioned above. It is also interesting to note that the full sample shows a stronger alignment than that of the LG sample. Since there is an alignment between $\hat{e}_3$ and $\hat{r}_{AB}$, in the following we will investigate the alignments of the distribution of satellites and of the dark substructures with $\hat{r}_{AB}$.

3.2. *Comparison between the satellite and the dark substructure distributions*

In the comparisons between observations and simulations, the plane-finding efforts have often been made in dark matter only simulations (Citar a Baumgartdt, Ibata, Pawlowsky cautun, buck etc...), and Sawalla et al. claims that once baryonic physics is included more planar distributions are found. We wanted to test if this holds true in the Illustris simulation, that also includes baryonic physics. So we first investigate if there is a difference in the bright and dark distribution in terms of their flatness. This flatness was quantified using the ratio of the semi-minor and semi-major axis of the triaxial distributions of both the bright satellite galaxies and the dark subhalos. In Figure 4 we can see the integrated probability of the axis ratios for the different halo pairs in both our full and LG samples. We find that indeed

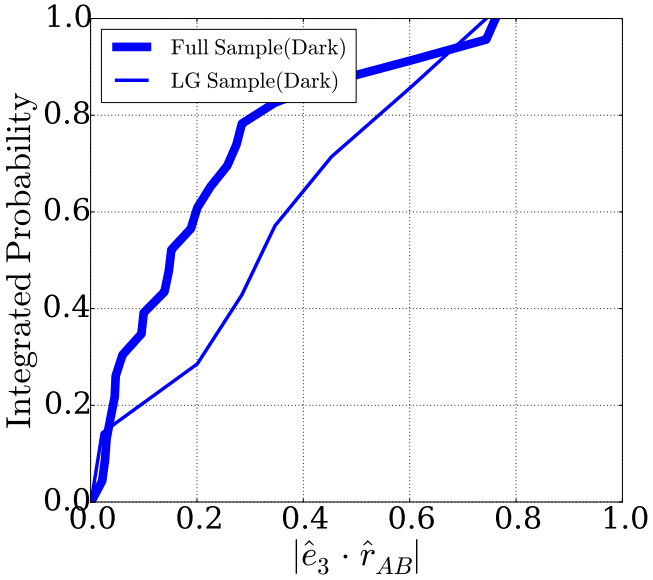

FIG. 3.— .

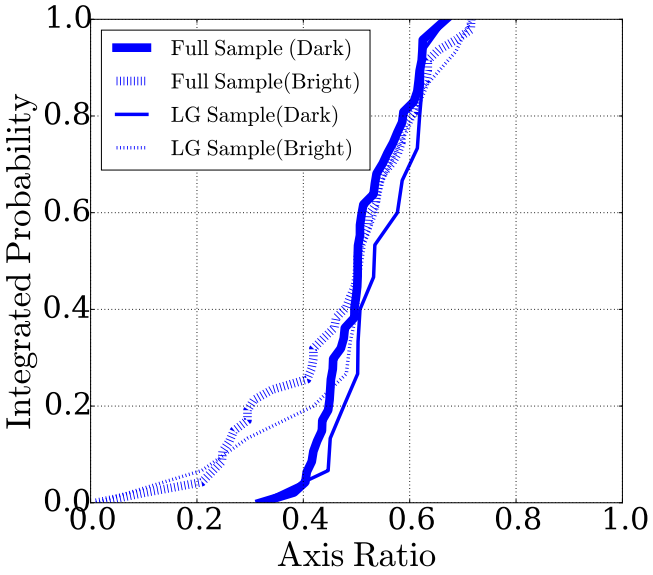

FIG. 4.— Axis ratio of luminous satellites versus the axis ratio for dark subhalos.

the bright distributions are flatter than the distributions that include also the dark substructure. This is in agreement with claims that the inclusion of baryonic physics results in more planar structures. However, this result alone is not enough to infer anything about the mechanisms behind the formation of these flatter distribution or if this increased flatness corresponds to the planes of satellite galaxies observed in the Local Group.

3.3. *Plane fitting: plane width versus object number*

We then fit planes to both the dark and bright distributions in order to test if it is indeed easier to find thinner planes in the bright distribution. We first fit planes to all the bright satellites for each halo in both the Full and LG samples and then repeat the process for the distributions that includes also the dark substructure. We then calculate the plane width of the best fit plane. In Figure 5 the integrated probability plot of the plane width for the different halo pairs shows that bright planes are thinner that dark planes in both our full and LG samples and the difference between the bright and dark distributions is starker than for the axis ratios. This again is in agreement with the idea that planes planes in simulations occur naturally when baryonic physics are included, but again this result alone is not enough to infer anything about the mechanisms behind their formation.

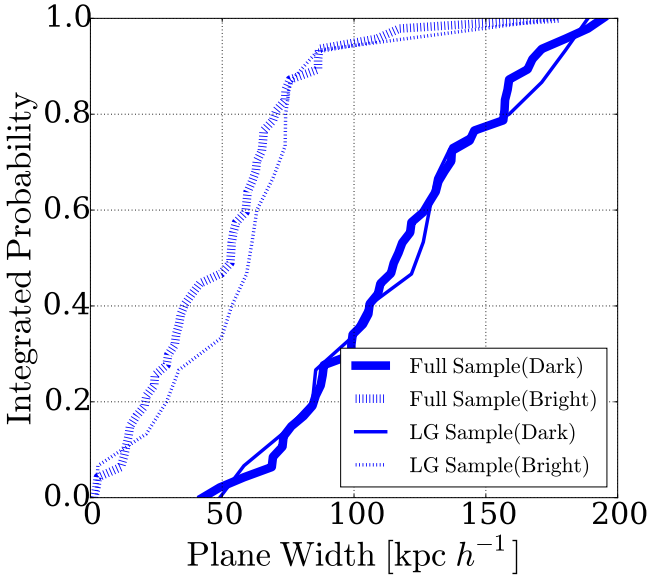

FIG. 5.— Plane width for the best planes in the luminious and dark cases.

To test if there is a physical reason for the difference in plane width between the bright and dark distributions or if this difference is due to a sampling effect, we look at the plane width as a function of number of objects in the plane. Since the bright satellites are a sub-sample of the dark distribution (that includes also the dark substructure), the number objects in "bright" planes is larger than that of "dark" planes for each given halo. In Figure 6 we can see that there is a strong correlation between the number of objects in the fitted plane and its width. Fewer objects are fitted by thinner planes. And in general, there are fewer brigth satellites, so the differences between the width of bright and dark distributions can be attributed to the number of objects and does not seem to be the result of other processes.

Icluir ac grficas de dark vs bright con el mismo numero?

3.4. *Alignments of the distributions with their environment*

From the comparison between the number of objects and the plane width we could conclude that there is not a physical mechanism behind the Local Group planar structures and that these are just due to the small number of satellites we observe. Nevertheless, these observed structures have, besides their special spatial configuration, a dynamical coherence that demands a better explanation for their formation mechanism (Pawlowski et al. 2014, Ibata et al. 2013 ...). Preferential accretion of the satellites and of the dark substructure has been explored as a possible formation mechanism of the ob-

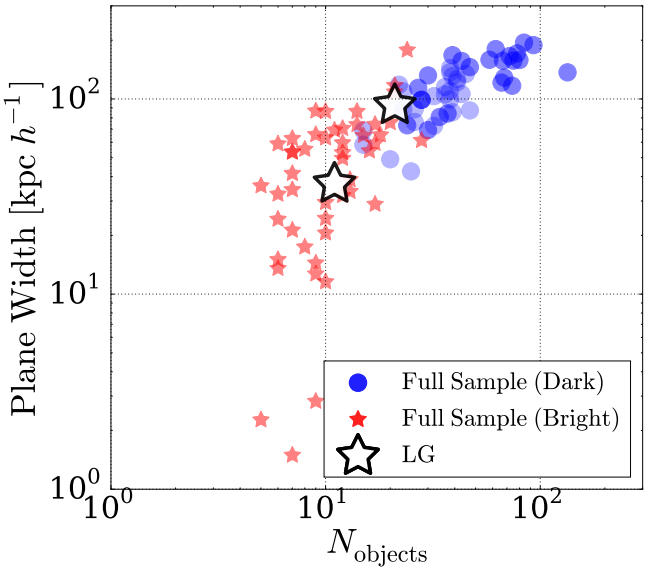

FIG. 6.— Plane width as a function of objects used to find the plane.

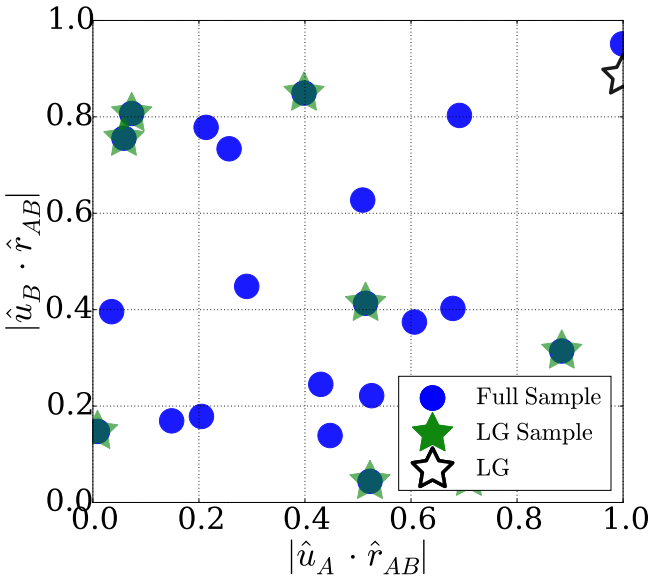

FIG. 7.— Alignment of the mayor axis with the vector connecting the two halos.

served Local Group planes of satellites. This mechanism would likely leave an imprint in the alignment between the distribution of satellites and dark substructure and the favoured accretion direction. In this work we study the alignment between the semi-major axis of the distribution and the axis that unites the halo pair. In Figure 7 we plot the dot product of the semimajor axis and the axis that unites the two halos unit vectors, for each halo pair in both sub-samples.

4. DISCUSSION

Difference between bright and dark distributions are only due to number.
We find significant alignments between distributions and H1H2 axis. But this alignments are the opposite as the one observed for the Local Group!!!

5. ACKNOWLEDGEMENTS

Gracias.

REFERENCES

Forero-Romero, J. E., & González, R. 2015, ApJ, 799, 45
Forero-Romero, J. E., Hoffman, Y., Bustamante, S., Gottlöber, S., & Yepes, G. 2013, ApJ, 767, L5
Forero-Romero, J. E., Hoffman, Y., Gottlöber, S., Klypin, A., & Yepes, G. 2009, MNRAS, 396, 1815
Hahn, O., Porciani, C., Carollo, C. M., & Dekel, A. 2007, MNRAS, 375, 489
Lee, J., & Choi, Y.-Y. 2015, ApJ, 799, 212
Libeskind, N. I., Guo, Q., Tempel, E., & Ibata, R. 2016, ArXiv e-prints
Libeskind, N. I., Knebe, A., Hoffman, Y., & Gottlöber, S. 2014, MNRAS, 443, 1274
Libeskind, N. I., Knebe, A., Hoffman, Y., Gottlöber, S., Yepes, G., & Steinmetz, M. 2011, MNRAS, 411, 1525
Lynden-Bell, D. 1976, MNRAS, 174, 695
Pawlowski, M. S., Famaey, B., Merritt, D., & Kroupa, P. 2015, ApJ, 815, 19
Pawlowski, M. S., Kroupa, P., Angus, G., de Boer, K. S., Famaey, B., & Hensler, G. 2012, MNRAS, 424, 80
Sawala, T., Frenk, C. S., Fattahi, A., Navarro, J. F., Bower, R. G., Crain, R. A., Dalla Vecchia, C., Furlong, M., Helly, J. C., Jenkins, A., Oman, K. A., Schaller, M., Schaye, J., Theuns, T., Trayford, J., & White, S. D. M. 2016, MNRAS, 457, 1931
Shao, S., Cautun, M., Frenk, C. S., Gao, L., Crain, R. A., Schaller, M., Schaye, J., & Theuns, T. 2016, ArXiv e-prints
Tempel, E., Guo, Q., Kipper, R., & Libeskind, N. I. 2015, MNRAS, 450, 2727

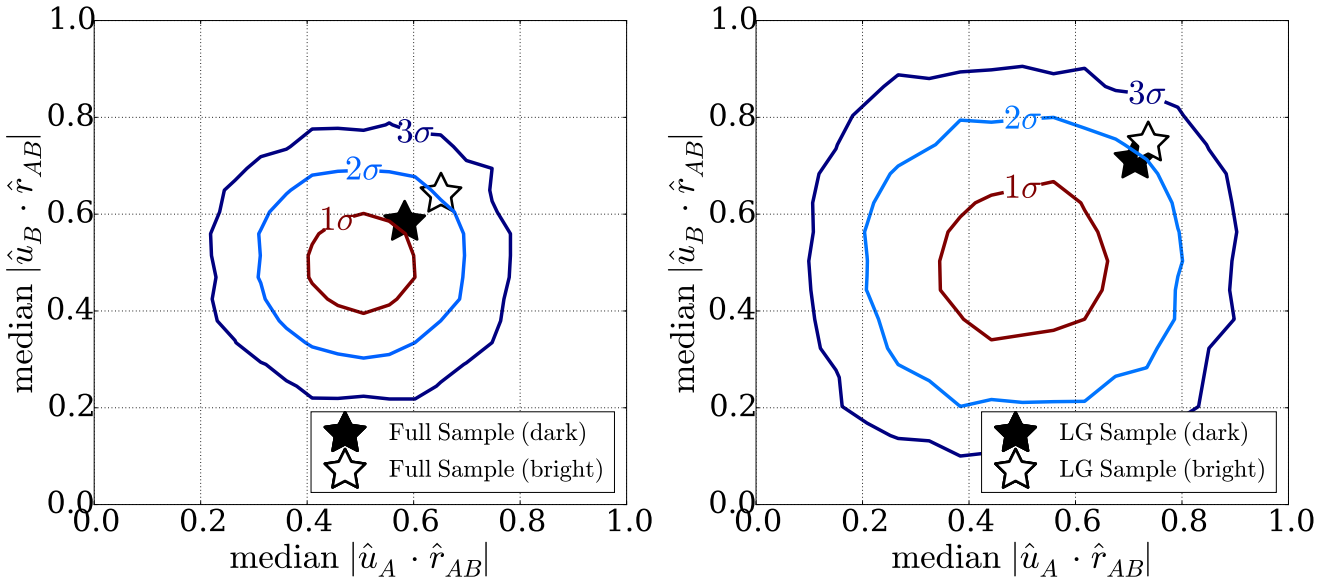

FIG. 8.— Significance of alignments for both samples.